

Calcareous nannofossils anchor chronologies for Arctic Ocean sediments back to 500 ka

Matt O'Regan¹, Jan Backman¹, Eliana Fornaciari², Martin Jakobsson¹ and Gabriel West¹

¹Department of Geological Sciences, Stockholm University, Stockholm SE-106 91, Sweden

²Department of Geosciences, University of Padova, Via G. Gradenigo, 6, 35131 Padova, Italy

ABSTRACT

Poor age control in Pleistocene sediments of the central Arctic Ocean generates considerable uncertainty in paleoceanographic reconstructions. This problem is rooted in the perplexing magnetic polarity patterns recorded in Arctic marine sediments and the paucity of microfossils capable of providing calibrated biostratigraphic biohorizons or continuous oxygen isotope stratigraphies. Here, we document the occurrence of two key species of calcareous nannofossils in a single marine sediment core from the central Arctic Ocean that provide robust, globally calibrated age constraints for sediments younger than 500 ka. The key species are the coccolithophores *Pseudoemiliana lacunosa*, which went extinct during marine isotope stage (MIS) 12 (478–424 ka), and *Emiliana huxleyi*, which evolved during MIS 8 (300–243 ka). This is the first time that *P. lacunosa* has been described in sediments of the central Arctic Ocean. The sedimentary horizons containing these age-diagnostic species can be traced, through lithostratigraphic correlation, across more than 450 km of the inner Arctic Ocean. They provide the first unequivocal support for proposed Pleistocene chronologies of sediment from this sector of the Arctic, and they constitute a foundation for developing and testing other geochronological tools for dating Arctic marine sediments.

INTRODUCTION

Arctic marine sediments can provide valuable paleoceanographic and paleoclimate time series documenting changes to the cryosphere across glacial cycles of the Pleistocene. Persistent challenges to dating Pleistocene Arctic sediments have hindered our ability to generate these time series (Backman et al., 2004; Alexanderson et al., 2014). These challenges arise from the sporadic downcore occurrence and limited diversity of microfossil assemblages, which result in few well-dated biostratigraphic datums and prevent the generation of a continuous and interpretable oxygen isotope stratigraphy (Backman et al., 2004). Compounding this problem, there is the complex sequence of high-frequency geomagnetic polarity reversals seen in many Arctic records (Clark, 1970; O'Regan et al., 2008; Xuan et al., 2012), which are difficult to reconcile with the geomagnetic polarity time scale or even with excursions in the Quaternary (Backman et al., 2008; Wiers et al., 2019). Due to these difficulties, proposed age models for Quaternary Arctic Ocean sediments have been debated since the 1970s (Backman et al., 2004; Hillaire-Marcel et al., 2017).

The occurrence of the calcareous nannofossil (coccolithophore) *Emiliana huxleyi* currently provides the most robust constraint on the age of Pleistocene Arctic Ocean sediments (Jakobsson et al., 2001; Backman et al., 2004, 2009), as this taxon evolved during marine isotope stage (MIS) 8 (300–243 ka) in both equatorial and subpolar environmental settings (Thierstein et al., 1977). In fact, the identification of *E. huxleyi* by Jakobsson et al. (2001) (core AO96/12–1PC, collected during the 1996 Arctic Ocean expedition on the icebreaker *Oden*, 87.0975°N, 144.7728°E; Fig. 1) in sediments previously dated to MIS 15 (621–563 ka) based on paleomagnetic interpretations (Spielhagen et al., 1997) finally illustrated that polarity reversals in near-surface Arctic sediments did not represent geomagnetic chron and subchron boundaries.

By combining downcore abundance patterns of calcareous nannofossils in core AO96/12–1PC (Fig. 1) and results from optically stimulated luminescence dating of quartz grains on a neighboring, stratigraphically correlated record (core AO96/24–1SEL, 87.1830°N, 144.6060°E; Jakobsson et al., 2003), the first appearance of *E. huxleyi* in the Arctic was argued to be during

the last interglacial period, MIS 5 (130–71 ka). This implied that while it evolved globally during MIS 8, it did not migrate into the Arctic until after the penultimate glaciation (MIS 6). The late Quaternary (MIS 7 to present) chronology developed for AO96/12–1PC (Jakobsson et al., 2000, 2001, 2003) underpins much of the subsequent paleoceanographic research in the Arctic (Spielhagen et al., 2004; O'Regan et al., 2008; Polyak et al., 2013; Cronin et al., 2019). The occurrence of *E. huxleyi* in AO96/12–1PC has even been used to age-calibrate recognized Arctic foraminiferal assemblage zones, like the *Bulimina aculeata* zone, which is now widely used to identify MIS 5 sediments from across the Arctic Ocean (Cronin et al., 2014).

The Pleistocene age model for the Integrated Ocean Drilling Program's Expedition 302, the Arctic Coring Expedition (ACEX, 87.8677°N, 136.1897°E; Fig. 1), built upon the late Quaternary chronology of core AO96/12–1PC by combining Neogene estimates of sedimentation rates derived from the decay of beryllium isotopes (¹⁰Be/⁹Be; Frank et al., 2008) with cyclostratigraphic analyses of lithologic changes in the upper 20 m of the borehole (O'Regan et al., 2008). The potential to generate cyclostratigraphic age models for Arctic sediments is grounded in the fact that downhole lithologic variability can be correlated across large spatial distances and clearly reflects oceanographic conditions across warmer and colder periods of Earth's past (Clark et al., 1980; Sellén et al., 2010; Schreck et al., 2018). However, lacking biostratigraphic support, and without age-depth tie points provided from paleomagnetic data, like the Brunhes-Matuyama boundary (781 ka), cyclostratigraphic approaches to age-model development that rely on lithologic variability (Jakobsson et al., 2000; O'Regan et al., 2008) or stacked records of microfossil abundances (Marzen et al., 2016) remain plagued by a high level of uncertainty. The magnitude of uncertainty can easily exceed

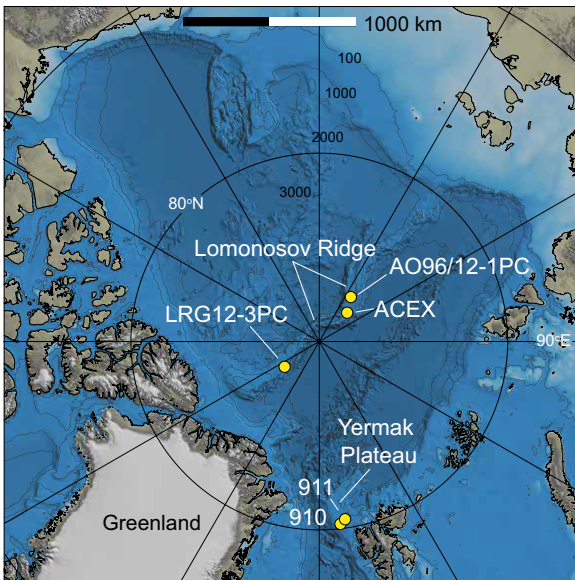


Figure 1. Map of the Arctic Ocean illustrating locations of key sediment cores discussed in the text. ACEX—Integrated Ocean Drilling Program’s Expedition 302, the Arctic Coring Expedition; 910, 911—Ocean Drilling Program Leg 151 Sites.

the length of 1–2 glacial cycles, due to relatively low and variable sedimentation rates and the ambiguity of differentiating interstadial/stadial from complete interglacial/glacial intervals.

Here, we present new results on the occurrence of two age-diagnostic taxa of calcareous nanofossils in a sediment core recovered from the central Arctic Ocean, between the northern Greenland margin and the geographic North Pole (Fig. 1). This is a region where downhole preservation of carbonate microfossils appears to be better than in other regions of the inner Arctic (Cronin et al., 2008; O’Regan et al., 2019). For the first time, we document in a single core the occurrence of *Pseudoemiliania lacunosa*, a species that went extinct during MIS

12, and the subsequent appearance of *E. huxleyi*, which evolved during MIS 8. This new data set allowed us to identify two critical globally calibrated Pleistocene biohorizons and evaluate these against the proposed age models for sediments on the Lomonosov Ridge (Jakobsson et al., 2000; O’Regan et al., 2008).

METHODS

During the joint Swedish-Danish Lomonosov Ridge off Greenland expedition in 2012 (LOMROG III) on icebreaker *Oden*, the 373-cm-long piston core LRG12–3PC (LRG = LomRoG) and the 57.5-cm-long trigger weight core (TWC) LRG12–3TWC were collected from 1607 m water depth on the Lomonosov Ridge (87.7247°N,

54.4253°W; Fig. 1). Previous work had dated the upper 30 cm of the TWC to MIS 3–MIS 1 using radiocarbon dating of planktic foraminifera (Chiu et al., 2017) and placed the complete core within the wider lithostratigraphic framework of sediments from the central Lomonosov Ridge (O’Regan et al., 2019).

We analyzed calcareous nanofossils in 46 discrete intervals of core LRG12–3PC, with samples targeting the dark-brown, bioturbated, finer-grained, Mn-enriched layers that are characteristic of interglacial/interstadial sediments from this region of the Arctic (Fig. 2; Jakobsson et al., 2000; O’Regan et al., 2008). Each smear slide was scanned in a light microscope using polarized light in 100 fields of view at 1600× magnification. This equates to a total scanning area of 2 mm². A minimum particle density of 100 grains that were 0.5 μm or larger was examined in each field of view, implying that between 10,000 and 15,000 particles were scanned in each smear slide.

RESULTS

Five major taxonomic categories were counted: *Emiliania huxleyi* (<4 μm), *Emiliania huxleyi* (>4 μm), *Gephyrocapsa caribbeanica* (near-closed center gephyrocapsids), *Gephyrocapsa muellerae* (open-center gephyrocapsids), and very small *Gephyrocapsa* (<2 μm, VSG) (Fig. 2; additional details are available in the Supplemental Material¹). Occasional specimens

¹Supplemental Material. Supplemental information with notes on taxonomy, and Figure S1 and Table S1 showing calcareous nanofossil abundances in core LRG12–3PC. Please visit <https://doi.org/10.1130/GEOL.S.12573995> to access the supplemental material, and contact editing@geosociety.org with any questions.

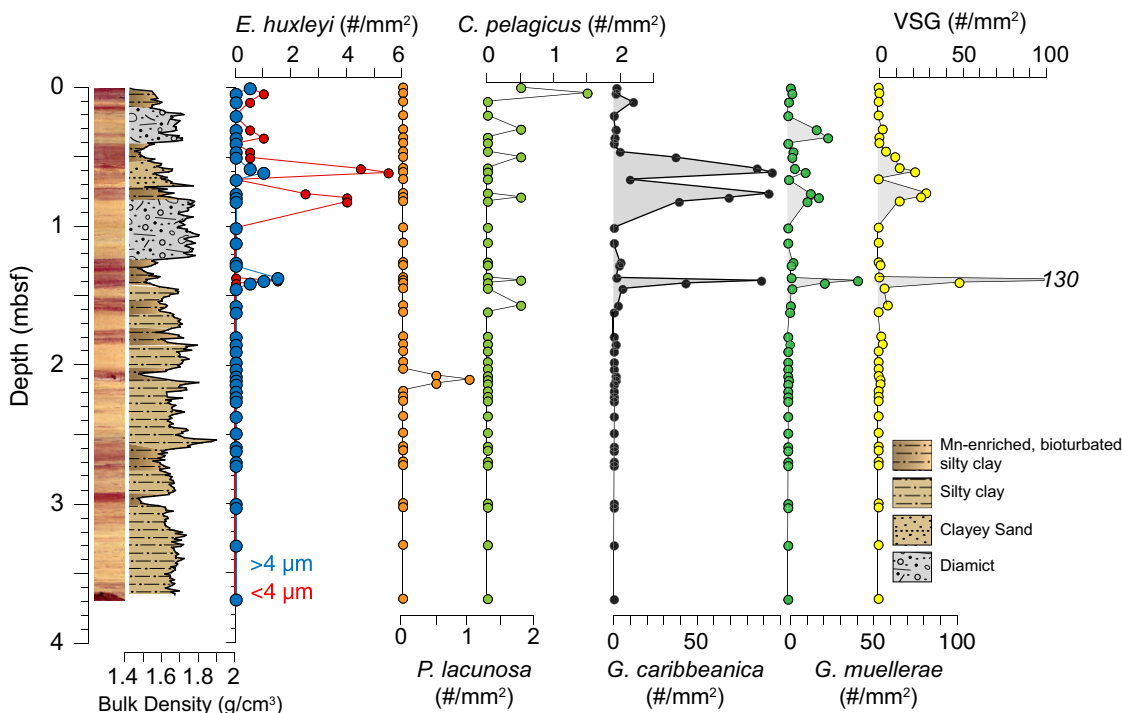


Figure 2. Core lithology and abundances of major taxonomic calcareous nanofossil categories in core LRG12–3PC (on the Lomonosov Ridge; 87.7247°N, 54.4253°W). Bulk density is proxy for grain-size variations (high bulk density = coarser-grained sediments) and is displayed alongside digital core image showing dark-brown, Mn-enriched bioturbated units associated with interglacial/interstadial sediments (mbsf—meters below seafloor). *E. huxleyi*—*Emiliania huxleyi*; *C. pelagicus*—*Coccolithus pelagicus*; *P. lacunosa*—*Pseudoemiliania lacunosa*; *G. caribbeanica*—*Gephyrocapsa caribbeanica*; *G. muellerae*—*Gephyrocapsa muellerae*; VSG—very small *Gephyrocapsa* (<2 μm).

of *Syracosphaera* spp., *Calcidiscus leptoporus*, and/or *Coccolithus pelagicus* as well as minor reworking of older Cenozoic and Mesozoic species, were also noted and are included in Table S1 in the Supplemental Material. All samples below 2.14 m below seafloor (mbsf) were barren of calcareous nannofossils.

The elliptical morphotype of *P. lacunosa* (sensu de Kaenel et al., 1999) occurred in three samples (2.08, 2.11, and 2.14 mbsf; Fig. 3). Searches in replicate smear slides from these levels generated identical results, attesting to the reproducibility of the results. Large (>4 μm) *E. huxleyi* specimens were observed in six samples, with three of these occurring over a 4 cm interval from 1.41 mbsf to 1.37 mbsf. The small (<4 μm) variety of *E. huxleyi* occurred in the intervening sample at 1.39 mbsf, together with *G. caribbeanica*, *G. muelleriae*, VSG, and *C. pelagicus* (Fig. 2; Table S1). This sample showed the highest abundances of calcareous nannofossils (527 specimens).

The interval from 0.82 mbsf to 0.50 mbsf was characterized by variable abundances of small *E. huxleyi* and gephyrocapsids, dominated by *G. caribbeanica*, and a few large *E. huxleyi* specimens. Calcareous nannofossils were less

common in the uppermost 0.46 mbsf interval, with relatively rare occurrences (11 specimens, including one large *E. huxleyi* specimen) in the core-top sample at 0.00 mbsf. This suggests that the Holocene may be largely missing in this core, as abundances of calcareous nannofossils tend to be high in Holocene Arctic sediments (Jakobsson et al., 2001).

DISCUSSION

The identification of *P. lacunosa* in LRG12–3PC marks its first reported occurrence in the inner Arctic Ocean. Previously, it was described in sediments from the Yermak Plateau (Ocean Drilling Program Leg 151, Sites 910 [80.2647°N, 6.5904°E] and 911 [80.4746°N, 8.2273°E]; Sato and Kameo, 1996) at the gateway for Atlantic water inflow to the Arctic (Fig. 1). It has a globally calibrated last occurrence in late MIS 12 (ca. 440 ka; Thierstein et al., 1977; Anthonissen and Ogg, 2012), providing an important biostratigraphic event for the later part (17% from top) of the Pleistocene (2.588–0.0118 Ma). It has provided important age control for previous paleoceanographic studies of the Yermak Plateau (Knies et al., 2007), and it can now be applied to central Arctic sediments as well.

A diagnostic feature of glacial/stadial sedimentary facies in the Arctic is the absence of microfossils. Since MIS 12 represents glacial conditions, we can assume that the observation of rare *P. lacunosa* in three adjacent samples (between 2.08 and 2.14 mbsf), together with gephyrocapsids, represents an interglacial prior to MIS 12, presumably MIS 13 (533–478 ka). The lack of calcareous nannofossils in two pre-MIS 13, bioturbated, Mn-enriched, dark-brown sediment layers (interglacials; Fig. 2) probably reflects carbonate dissolution.

There is a remarkable consistency in down-core lithologic changes in many marine sediment cores collected along the Lomonosov Ridge (Löwemark et al., 2014; O'Regan et al., 2019). This includes the recurrent pattern of dark-brown, Mn-enriched, bioturbated intervals, and two pronounced diamicts found in the upper interval of many cores (Fig. 4). The lower diamict was deposited during MIS 6, an assertion supported by optically stimulated luminescence dating of the overlying interglacial sediments (Jakobsson et al., 2003). Using this regional lithostratigraphic correlation, we can compare the new calcareous nannofossil data from LRG12–3PC with proposed age models for ACEX (O'Regan et al., 2008) and AO96/12–1PC (Jakobsson et al., 2000). These age models are consistent back to MIS 14/15 (563 ka; O'Regan et al., 2008) and were generated using lithology-based cyclostratigraphic alignment to global benthic $\delta^{18}\text{O}$ records (Lisiecki and Raymo, 2005). Neither of these age models contains independently dated tie points below MIS 5, although the ACEX age model provisionally iden-

tified the Brunhes-Matuyama boundary within a more complex sequence of apparent magnetic polarity reversals (O'Regan et al., 2008). Critically, in LRG12–3PC, the inferred MIS 13 age based on the occurrence of *P. lacunosa* is consistent with proposed age models in these neighboring records (Fig. 4). This provides the first independently calibrated support predating MIS 5 for Pleistocene age models in the central Arctic Ocean.

Equally important factors for anchoring these age models are the occurrences of *E. huxleyi* farther up core. Many previous studies have observed late Pleistocene occurrences of large (>4 μm) *E. huxleyi* specimens, including from the Arctic Ocean (Backman et al., 2009). This form is considered to represent a cold-water variety (Colmenero-Hidalgo et al., 2002) that evolved simultaneously with the smaller (<4 μm) forms during the later part of MIS 8 (Balestra et al., 2015). Because MIS 8 represents glacial conditions, it can be assumed that Arctic sediments would lack calcareous nannofossils due to heavy sea-ice cover. The observation of rare *E. huxleyi* in three samples (1.41–1.39–1.37 mbsf), together with peak abundances of gephyrocapsids (Fig. 2), is therefore interpreted to represent an interglacial younger than MIS 8, presumably MIS 7 (243–191 ka).

The lowermost occurrence of *E. huxleyi* (1.39 \pm 0.02 mbsf) in LRG12–3PC during MIS 7 is consistent with dating of the overlying diamict to MIS 6 (Fig. 4; Jakobsson et al., 2003). Furthermore, two interglacial/interstadial facies (bioturbated, dark-brown units) exist between the highest occurrence of *P. lacunosa* (MIS 13) and the lowest occurrence of *E. huxleyi* (MIS 7), allowing us to confidently assign these units to MIS 11 and MIS 9, respectively (Fig. 4), and providing additional support for these being accurate age-diagnostic occurrences of these taxa.

Higher abundances of *E. huxleyi* occur above the MIS 6 diamict between 0.82 and 0.58 mbsf (Figs. 3 and 4). These occurrences are consistent with its prevalence in other Arctic Ocean records during MIS 5 (Jakobsson et al., 2001; Backman et al., 2009). The downcore abundance patterns of *E. huxleyi* in LRG12–3PC now clearly indicate that its first appearance in the Arctic was nearly coeval with its evolution in the global oceans, occurring in MIS 7 rather than MIS 5, where it has been most commonly identified (Jakobsson et al., 2001; Alexanderson et al., 2014). This does not imply that the age model for AO96/12–1PC was incorrect, simply that the lowermost assemblage of calcareous nannofossils assigned to MIS 7 did not contain *E. huxleyi* (Fig. S1). Due to the generally low numbers of *E. huxleyi* reported in most Arctic records, its absence in sediments older than MIS 6 (i.e., AO96/12–1PC) may be a local environmental signal, an artifact of dissolution, or a sign that occurrence-

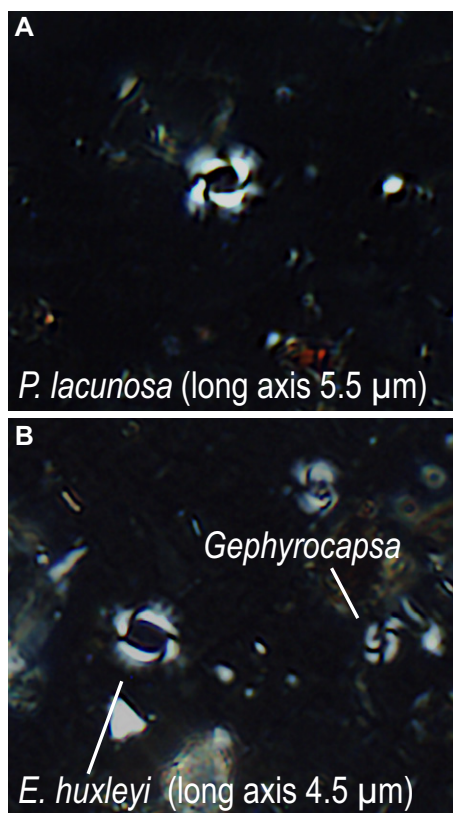


Figure 3. Light microscope images of (A) elliptical morphotype of *Pseudoemiliania lacunosa* (core LRG12–3PC [87.7247°N, 54.4253°W], Section 2, 138 cm, 2.11 meters below seafloor [mbsf]), and (B) large (>4 μm) *Emiliana huxleyi* and *Gephyrocapsa* specimens (LRG12–3PC, Section 2, 66 cm, 1.39 mbsf).

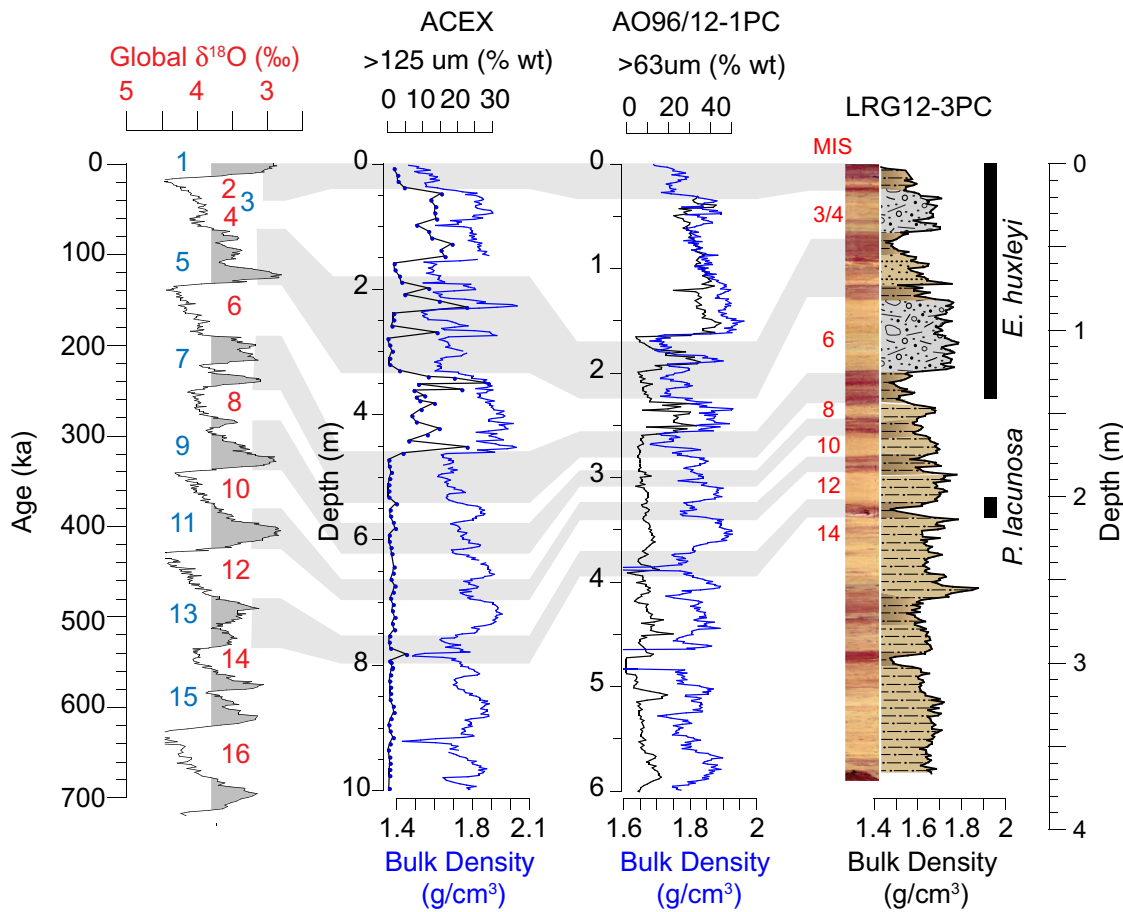


Figure 4. Litho- and chronostratigraphic correlation of core AO96/12-1PC (87.0975°N, 144.7728°E), the Arctic Coring Expedition (ACEX) composite core (87.8677°N, 136.1897°E), and core LRG12-3PC (87.7247°N, 54.4253°W). Consistent lithostratigraphic correlations between these records have been illustrated using various lithologic proxies (O'Regan et al., 2019). Published cyclostratigraphic age model extending back to marine isotope stage (MIS) 14 for ACEX is shown against the global benthic $\delta^{18}\text{O}$ record (Lisiecki and Raymo, 2005). *E. huxleyi*—*Emiliana huxleyi*; *P. lacunosa*—*Pseudoemiliana lacunosa*.

es may have been overlooked. In this regard, it is worth noting that despite the proximity of records like ACEX and AO96/12-1PC, there is a large difference in the preservation of calcareous nannofossils. High abundances were found in MIS 5 sediments in AO96/12-1PC, while no nannofossils were preserved in stratigraphically coeval sediments at ACEX.

Whatever the underlying reason for its absence in other records, occurrences of *E. huxleyi* in LRG12-3PC now bracket the lower diamic, providing additional support for its age assignment to MIS 6 (Fig. 4), when a kilometer-thick ice shelf was grounded on many bathymetric highs of the central Arctic Ocean (Jakobsson et al., 2016), although uncertainty remains about when during MIS 6 this ice shelf broke up (Stein et al., 2017).

Sedimentation rates in LRG12-3PC are substantially lower than those found at ACEX and in AO96/12-1PC (Fig. 4). This precludes a more detailed analysis that could help delineate the exact MIS boundaries, but it provides a robust chronological framework that can be applied to other records from the area, and that can be used to test other geochronological tools for dating Arctic Ocean sediments. Furthermore, there remains some uncertainty in the placement of boundaries for MIS 3/4 and MIS 4/5 across the Lomonosov Ridge that still needs to be resolved.

CONCLUSIONS

In a sediment core from the central Arctic Ocean, we documented the occurrence of two calcareous nannofossil taxa that have globally calibrated biozonations. We used these to anchor the chronology of sediments over the past 500 k.y. (MIS 13–5). The resulting age model is in agreement with previously published cyclostratigraphic age models for Lomonosov Ridge sediments that predate MIS 6. This presents a significant step forward in Arctic Pleistocene geochronology, allowing us to confidently move forward with detailing environmental changes in the Arctic across glacial cycles of the later Pleistocene.

ACKNOWLEDGMENTS

Reviews by Robert Spielhagen and an anonymous reviewer improved the manuscript and are gratefully acknowledged. Financial support for this work was provided to O'Regan by the Swedish Research Council (VR) (Project Number DNR-2016-05092). We thank the Swedish Polar Secretariat and the captain and crew of *I/B Oden* who made data collection on the expedition possible.

REFERENCES CITED

- Alexanderson, H., et al., 2014, An Arctic perspective on dating mid-late Pleistocene environmental history: *Quaternary Science Reviews*, v. 92, p. 9–31, <https://doi.org/10.1016/j.quascirev.2013.09.023>.
- Anthonissen, D.E., and Ogg, J.G., 2012, Appendix 3—Cenozoic and Cretaceous biochronology

of planktonic foraminifera and calcareous nannofossils, in Gradstein, F.M., et al., eds., *The Geological Time Scale 2012*: Amsterdam, Netherlands, Elsevier, p. 1083–1127, <https://doi.org/10.1016/B978-0-444-59425-9.15003-6>.

- Backman, J., Jakobsson, M., Løvlie, R., Polyak, L., and Febo, L.A., 2004, Is the central Arctic Ocean a sediment starved basin?: *Quaternary Science Reviews*, v. 23, p. 1435–1454, <https://doi.org/10.1016/j.quascirev.2003.12.005>.
- Backman, J., et al., 2008, Age model and core-seismic integration for the Cenozoic ACEX sediments from the Lomonosov Ridge: *Paleoceanography*, v. 23, PA1S03, <https://doi.org/10.1029/2007PA001476>.
- Backman, J., Fornaciari, E., and Rio, D., 2009, Biochronology and paleoceanography of late Pleistocene and Holocene calcareous nannofossil abundances across the Arctic Basin: *Marine Micropaleontology*, v. 72, p. 86–98, <https://doi.org/10.1016/j.marmicro.2009.04.001>.
- Balestra, B., Flores, J.-A., Hodell, D.A., Hernández-Molina, F.J., and Stow, D.A.V., 2015, Pleistocene calcareous nannofossil biochronology at IODP Site U1385 (Expedition 339): *Global and Planetary Change*, v. 135, p. 57–65, <https://doi.org/10.1016/j.gloplacha.2015.10.004>.
- Chiu, P.-Y., Chao, W.-S., Gyllencreutz, R., Jakobsson, M., Li, H.-C., Löwemark, L., and O'Regan, M., 2017, New constraints on Arctic Ocean Mn stratigraphy from radiocarbon dating on planktonic foraminifera: *Quaternary International*, v. 447, p. 13–26, <https://doi.org/10.1016/j.quaint.2016.11.030>.
- Clark, D.L., 1970, Magnetic reversals and sedimentation rates in the Arctic Ocean: *Geological Society of America Bulletin*, v. 81, p. 3129–3134, <https://doi.org/10.1016/j.gloplacha.2015.10.004>.

- doi.org/10.1130/0016-7606(1970)81[3129:MRASRJ]2.0.CO;2.
- Clark, D.L., Whitman, R.R., Morgan, K.A., and Mackey, S.D., 1980, Stratigraphy and Glacial-Marine Sediments of the Amerasian Basin, Central Arctic Ocean: Geological Society of America Special Papers, v. 181, 57 p., <https://doi.org/10.1130/SPE181>.
- Colmenero-Hidalgo, E., Flores, J.-A., and Siero, F.J., 2002, Biometry of *Emiliania huxleyi* and its biostratigraphic significance in the eastern North Atlantic Ocean and Western Mediterranean Sea in the last 20 000 years: *Marine Micropaleontology*, v. 46, p. 247–263, [https://doi.org/10.1016/S0377-8398\(02\)00065-8](https://doi.org/10.1016/S0377-8398(02)00065-8).
- Cronin, T., Eynaud, F., Smith, S., O'Regan, M., and King, J., 2008, Quaternary paleoceanography of the central Arctic based on IODP ACEX 302 foraminiferal assemblages: *Paleoceanography*, v. 23, PA1S18, <https://doi.org/10.1029/2007PA001484>.
- Cronin, T.M., DeNinno, L.H., Polyak, L., Caverly, E.K., Poore, R.Z., Brenner, A., Rodriguez-Lazaro, J., and Marzen, R.E., 2014, Quaternary ostracode and foraminiferal biostratigraphy and paleoceanography in the western Arctic Ocean: *Marine Micropaleontology*, v. 111, p. 118–133, <https://doi.org/10.1016/j.marmicro.2014.05.001>.
- Cronin, T.M., et al., 2019, Interglacial paleoclimate in the Arctic: *Paleoceanography and Paleoclimatology*, v. 34, p. 1959–1979, <https://doi.org/10.1029/2019PA003708>.
- de Kaenel, E., Siesser, W.G., and Murat, A., 1999, Pleistocene calcareous nannofossil biostratigraphy and the Western Mediterranean sapropels, Sites 974 to 977 and 979, in Zahn, R., et al., Proceedings of the Ocean Drilling Program, Scientific Results, Leg 161: College Station, Texas, Ocean Drilling Program, p. 159–183, <https://doi.org/10.2973/odp.proc.sr.161.250.1999>.
- Frank, M., Backman, J., Jakobsson, M., Moran, K., O'Regan, M., King, J., Haley, B. A., Kubik, P. W., and Garbe-Schönberg, D., 2008, Beryllium isotopes in central Arctic Ocean sediments over the past 12.4 million years: Stratigraphic and paleoceanographic implications: *Paleoceanography*, v. 23, PA1S02, <https://doi.org/10.1029/2007PA001478>.
- Hillaire-Marcel, C., Ghaleb, B., de Vernal, A., Maccali, J., Cuny, K., Jacobel, A., Le Duc, C., and McManus, J., 2017, A new chronology of late Quaternary sequences from the central Arctic Ocean based on “extinction ages” of their excesses in ^{231}Pa and ^{230}Th : *Geochemistry Geophysics Geosystems*, v. 18, p. 4573–4585, <https://doi.org/10.1002/2017GC007050>.
- Jakobsson, M., Løvlie, R., Al-Hanbali, H., Arnold, E., Backman, J., and Mörth, M., 2000, Manganese and color cycles in Arctic Ocean sediments constrain Pleistocene chronology: *Geology*, v. 28, p. 23–26, [https://doi.org/10.1130/0091-7613\(2000\)28<23:MACCIA>2.0.CO;2](https://doi.org/10.1130/0091-7613(2000)28<23:MACCIA>2.0.CO;2).
- Jakobsson, M., Løvlie, R., Arnold, E.M., Backman, J., Polyak, L., Knutsen, J.O., and Musatov, E., 2001, Pleistocene stratigraphy and paleoenvironmental variation from Lomonosov Ridge sediments, central Arctic Ocean: *Global and Planetary Change*, v. 31, p. 1–22, [https://doi.org/10.1016/S0921-8181\(01\)00110-2](https://doi.org/10.1016/S0921-8181(01)00110-2).
- Jakobsson, M., Backman, J., Murray, A., and Løvlie, R., 2003, Optically stimulated luminescence dating supports central Arctic Ocean cm-scale sedimentation rates: *Geochemistry Geophysics Geosystems*, v. 4, 1016, <https://doi.org/10.1029/2002GC000423>.
- Jakobsson, M., et al., 2016, Evidence for an ice shelf covering the central Arctic Ocean during the penultimate glaciation: *Nature Communications*, v. 7, p. 10365, <https://doi.org/10.1038/ncomms10365>.
- Knies, J., Matthiessen, J., Mackensen, A., Stein, R., Vogt, C., Frederichs, T., and Nam, S.-I., 2007, Effects of Arctic freshwater forcing on thermohaline circulation during the Pleistocene: *Geology*, v. 35, p. 1075–1078, <https://doi.org/10.1130/G23966A.1>.
- Lisiecki, L., and Raymo, M., 2005, A Pliocene–Pleistocene stack of 57 globally distributed benthic $\delta^{18}\text{O}$ records: *Paleoceanography*, v. 20, PA1003, <https://doi.org/10.1029/2004PA001071>.
- Löwemark, L., März, C., O'Regan, M., and Gyllencreutz, R., 2014, Arctic Ocean Mn-stratigraphy: Genesis, synthesis and inter-basin correlation: *Quaternary Science Reviews*, v. 92, p. 97–111, <https://doi.org/10.1016/j.quascirev.2013.11.018>.
- Marzen, R.E., DeNinno, L.H., and Cronin, T.M., 2016, Calcareous microfossil-based orbital cyclostratigraphy in the Arctic: *Quaternary Science Reviews*, v. 149, p. 109–121, <https://doi.org/10.1016/j.quascirev.2016.07.004>.
- O'Regan, M., King, J., Backman, J., Jakobsson, M., Pälike, H., Moran, K., Heil, C., Sakamoto, T., Cronin, T.M., and Jordan, R.W., 2008, Constraints on the Pleistocene chronology of sediments from the Lomonosov Ridge: *Paleoceanography*, v. 23, PA1S19, <https://doi.org/10.1029/2007PA001551>.
- O'Regan, M., Coxall, H.K., Cronin, T.M., Gyllencreutz, R., Jakobsson, M., Kaboth, S., Löwemark, L., Wiers, S., and West, G., 2019, Stratigraphic occurrences of sub-polar planktic foraminifera in Pleistocene sediments on the Lomonosov Ridge, Arctic Ocean: *Frontiers of Earth Science*, v. 7, 71, <https://doi.org/10.3389/feart.2019.00071>.
- Polyak, L., Best, K.M., Crawford, K.A., Council, E.A., and St-Onge, G., 2013, Quaternary history of sea ice in the western Arctic Ocean based on foraminifera: *Quaternary Science Reviews*, v. 79, p. 145–156, <https://doi.org/10.1016/j.quascirev.2012.12.018>.
- Sato, T., and Kameo, K., 1996, Pliocene to Quaternary calcareous nannofossil biostratigraphy of the Arctic Ocean, with reference to late Pliocene glaciation, in Thiede, J., et al., Proceedings of the Ocean Drilling Program, Scientific Results, Leg 151: College Station, Texas, Ocean Drilling Program, p. 39–59, <https://doi.org/10.2973/odp.proc.sr.151.112.1996>.
- Schreck, M., Nam, S.-I., Polyak, L., Vogt, C., Kong, G.S., Stein, R., Matthiessen, J., and Niessen, F., 2018, Improved Pleistocene sediment stratigraphy and paleoenvironmental implications for the western Arctic Ocean off the East Siberian and Chukchi margins: *Arktos*, v. 4, p. 21, <https://doi.org/10.1007/s41063-018-0057-8>.
- Sellén, E., O'Regan, M., and Jakobsson, M., 2010, Spatial and temporal Arctic Ocean depositional regimes: A key to the evolution of ice drift and current patterns: *Quaternary Science Reviews*, v. 29, p. 3644–3664, <https://doi.org/10.1016/j.quascirev.2010.06.005>.
- Spielhagen, R.F., et al., 1997, Arctic Ocean evidence for late Quaternary initiation of northern Eurasian ice sheets: *Geology*, v. 25, p. 783–786, [https://doi.org/10.1130/0091-7613\(1997\)025<0783:AOEFLQ>2.3.CO;2](https://doi.org/10.1130/0091-7613(1997)025<0783:AOEFLQ>2.3.CO;2).
- Spielhagen, R.F., Baumann, K.-H., Erlenkeuser, H., Nowaczyk, N.R., Nørgaard-Pedersen, N., Vogt, C., and Weiel, D., 2004, Arctic Ocean deep-sea record of northern Eurasian ice sheet history: *Quaternary Science Reviews*, v. 23, p. 1455–1483, <https://doi.org/10.1016/j.quascirev.2003.12.015>.
- Stein, R., Fahl, K., Gierz, P., Niessen, F., and Lohmann, G., 2017, Arctic Ocean sea ice cover during the penultimate glacial and the last interglacial: *Nature Communications*, v. 8, p. 373, <https://doi.org/10.1038/s41467-017-00552-1>.
- Thierstein, H.R., Geitzenauer, K.R., Molino, B., and Shackleton, N.J., 1977, Global synchronicity of late Quaternary coccolith datum levels: Validation by oxygen isotopes: *Geology*, v. 5, p. 400–404, [https://doi.org/10.1130/0091-7613\(1977\)5<400:GSOLQC>2.0.CO;2](https://doi.org/10.1130/0091-7613(1977)5<400:GSOLQC>2.0.CO;2).
- Wiers, S., Snowball, I., O'Regan, M., and Almqvist, B., 2019, Late Pleistocene chronology of sediments from the Yermak Plateau and uncertainty in dating based on geomagnetic excursions: *Geochemistry Geophysics Geosystems*, v. 20, p. 3289–3310, <https://doi.org/10.1029/2018GC007920>.
- Xuan, C., Channell, J.E.T., Polyak, L., and Darby, D.A., 2012, Paleomagnetism of Quaternary sediments from Lomonosov Ridge and Yermak Plateau: Implications for age models in the Arctic Ocean: *Quaternary Science Reviews*, v. 32, p. 48–63, <https://doi.org/10.1016/j.quascirev.2011.11.015>.

Printed in USA